

PS2 / Latest Techniques in Asset Management,
Capacity Enhancement, Refurbishment**Evaluation of long-term reliability of the carbon fiber core wire and
development of technologies to expand its application****Hiroaki SASA***
Tohoku Electric Power
Network Co., Inc.
Japan

sasa.hiroaki.hy@tohoku-epco.co.jp

Tomoyuki AOYAMA
Tohoku Electric Power
Network Co., Inc.
Japan

aoyama.tomoyuki.hc@tohoku-epco.co.jp

Naohiko SUDO
Tohoku Electric Power
Network Co., Inc.
Japan

sudo.naohiko.fs@tohoku-epco.co.jp

Kiyonobu NARA
Kitanihon Electric
Cable Co., Ltd.
Japan

nara@kitaniti-td.co.jp

Takao KANEKO
Fujikura Ltd.
Japan

takao.kaneko@jp.fujikura.com

Mami NAKAGAWA
Furukawa Electric Power
Systems Co., Ltd.
Japan

mami.nakagawa@furukawaelectric.com

SUMMARY

In order to increase conductor clearance above ground in urban areas, methods to reconstruct or raise the tower have been adopted. However, when using these methods, the construction cost is increased due to the restriction of land use for working space and the limitation of working on site. Therefore, in 2002, the authors developed an Aluminum Conductor Fiber Reinforced (hereinafter, ACFR), which uses a Carbon Fiber Composite Cable (hereinafter, CFCC) instead of a conventional steel core, in order to increase conductor clearance above ground.

The demand for ACFR has been increasing in recent years because replacing the ACSR with the thermal-resistant ACFR (TACFR) can reduce conductor sag and increase transmission capacity without reconstructing existing transmission towers.

The authors had installed ACFR on a 66 kV transmission line about 8 km from the coast for 16 years from December 2002 to January 2019. Subsequently, various evaluation tests were conducted to evaluate the reliability of the ACFR and the compression-type dead-end clamp that had been used over a long-term service of overhead lines. As a result, it was judged that ACFR can be used without any problem during the life of the transmission facility because no significant deterioration was observed and the tensile load tended to slightly decrease. No significant degradation was also observed for the compression-type dead-end clamp.

Furthermore, the authors have developed SBTACFR (SB: Smooth Body), in which the aluminum strand is formed into a trapezoidal shape to enlarge the cross-sectional area of the aluminum portion, thus reducing power losses and increasing the transmission capacity. In addition, we have developed a compression-type dead-end clamp, which passes through a sheave, making it possible to reduce the work time required for compression on the tower. And the application of counterweights to suppress heavy snow accumulation on overhead lines and anti-vibration dampers to suppress the wind vibration of transmission lines was verified and no problems were found. As a result, the expansion of the application of ACFR has been foreseen.

KEYWORDS

HTLS, ACFR, TACFR, CFCC, Composite-conductor, Long term reliability evaluation, Fitting

1. INTRODUCTION

As a countermeasure to increase conductor clearance above ground due to the urbanization of areas around overhead transmission lines, the reconstruction of towers and the raising of existing towers have been carried out in the past. However, the implementation of these measures is subject to restrictions such as site constraints and work during stopping power supply, which increase the construction cost. In 2002, the authors developed an ACFR that uses CFCC instead of conventional steel cores in order to secure the conductor clearance above ground by replacing the conductors with ones with less sagging. CFCC is composed of 10,000 to 12,000 filaments with diameters between 5 to 7 μm , which are grouped and covered with a thermosetting resin. It is very light, its mass roughly about 1/5 of a steel core of the same diameter, and has a lower thermal expansion coefficient, approximately 1/10 of a steel core. It has a 30-40% higher mechanical strength than the steel core of an equivalent cross-section, is electrically inert, and has no magnetic losses. It has the flexibility equivalent of a steel core, and is corrosion-resistant to acid, water and ultraviolet rays, and is highly resistant to vibration fatigue [1]. CFCC has many useful features compared to the conventional steel core.

2. ACSR AND ACFR SPECIFICATIONS AND THEIR SAG AND TEMPERATURE CHARACTERISTICS

Table I shows the specifications of ACSR and ACFR [2]. Fig. 1 shows the appearance of ACFR [2]. Although ACSR and ACFR have the same shape, ACFR are about 30% lighter than ACSR in terms of conductor weight of the same size. In addition, the thermal expansion coefficient of ACFR decreases by about 1/10 at its high temperature working areas where sagging is a problem. This leads ACFR to suppress conductor sagging.

Table I Specifications of ACSR and ACFR

Item		Characteristics	
Conductor		ACSR	ACFR
Nominal cross section (mm^2)		160	160
Working Temperature ($^{\circ}\text{C}$)	Continuous	90 (TACSR 150)	90 (TACFR 150)
	Short-time	120 (TACSR 180)	120 (TACFR 180)
Strands (Number/mm)	Aluminum	30/2.6	30/2.6
	Core	7/2.6	7/2.6
DC resistance at 20°C (Ω/km)		0.182 (TACSR 0.185)	0.182 (TACFR 0.185)
Continuous current capacity (A)		454 (TACSR 705)	454 (TACFR 705)
Calculated cross section (mm^2)		196.5	196.5
Outer diameter (mm)		18.2	18.2
Weight (kg/km)		732.8	502.5
Tensile load (kN)		68.4	68.9
Modulus of elasticity (GPa)	Below transition temp.	89.1	76.0
	Above transition temp.	206	137
Thermal expansion coefficient ($\times 10^{-6}/^{\circ}\text{C}$)	Below transition temp.	18.0	15.5
	Above transition temp.	11.5	1.0

* The wire specifications of TACSR and TACFR are shown in (). Values without () are the same as ACSR or ACFR.

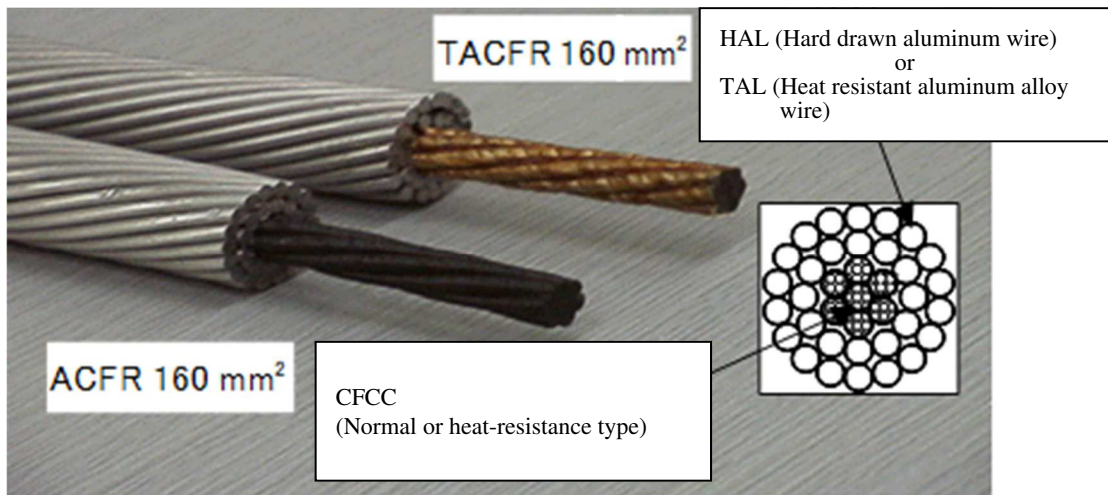


Fig. 1 Appearance of the ACFR

A comparison of sag/temperature characteristics of ACSR and ACFR is shown in Fig. 2. With a span length of 300 m, the sag at 90°C, which is the continuous allowable temperature of a normal type conductor, is 9.3 m for ACFR while it is 11.3 m for ACSR. This indicates that ACFR can suppress sag by approx. 2.0 m.

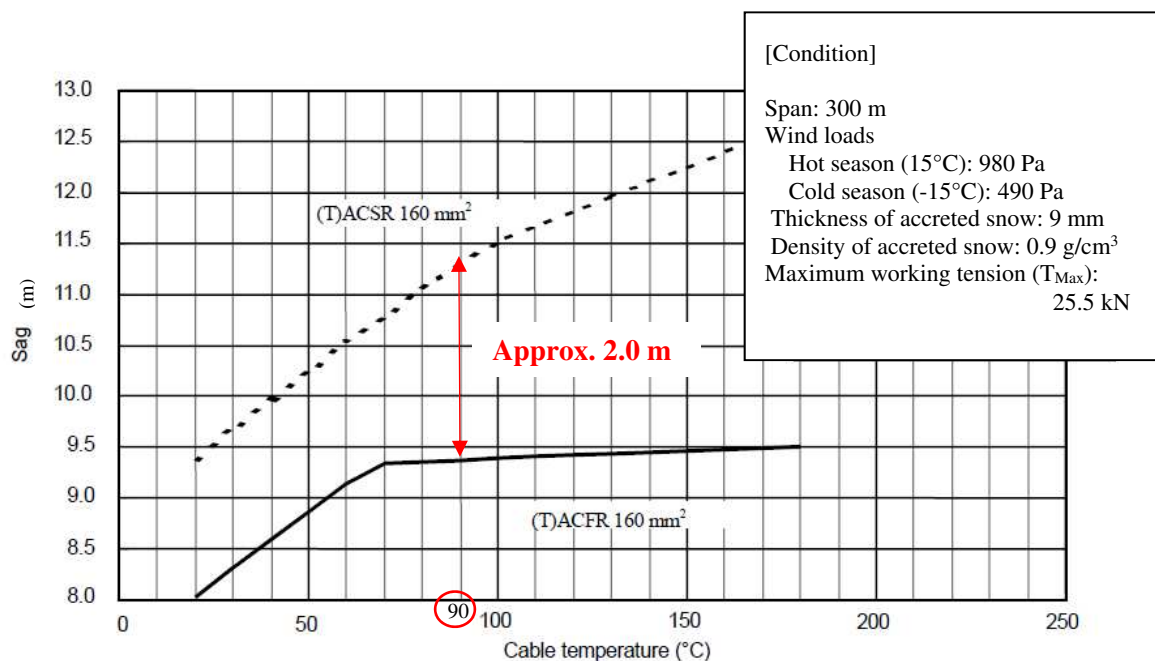


Fig. 2 Comparison of sag/temperature characteristics of ACSR and ACFR

3. LONG-TERM RELIABILITY EVALUATION OF ACFR AND COMPRESSION-TYPE DEAD-END CLAMP

In order to evaluate the reliability of ACFR and the compression-type dead-end clamp over a long-term service of overhead lines, samples were taken from ACFR and clamps that had been installed on a 66 kV transmission line at a distance of about 8 km from the coast for about 16 years from December 2002 to January 2019, and various evaluation tests were conducted.

3.1 Overview of the performance evaluation test

3.1.1 Sample Summary of the performance evaluation test

Table II shows the sample summary of the various evaluation tests.

Table II Sample Summary

Sample	Electric conductor		Compression clamp
Date collected	January 2019		
Transmission line	66kV transmission line (1 circuit) / ACFR was installed at 4 span.		
Conductor type and size	ACFR 160 mm ²		
Date of wire installation	December 2002		
Number of years passed	16 years and 1 month		
Estimated maximum salt attachment density	0.25 (mg/cm ²) / The span used by the ACFR was located about 8 km from the coast.		
Sample quantity	60 m	30 m	3 sets
Sample location	Lowest part of the sag	Suspension clamp, damper grip	1 steel tower

3.1.2 Test items and quantities

Table III shows the test items and quantities for the conductor, and Table IV shows the test items and quantities for the compression clamps. The test items for conductor were set up to check for changes in the composition of CFCC at the lowest part of the sag, where rainwater tends to accumulate, and to check for degradation of the strength and damage of CFCC due to the vibration of the suspension device and conductor at the gripping area of the suspension clamps or dampers.

Table III Test items and quantities for conductor

Line type	Test Items	Test quantity	Bottom of sagging	Suspension clamp gripping area	Damper gripping area
Hard aluminum wire	All items*	all	all		
CFCC	Appearance and structure	n=1	n=1		
	Tensile load	n=2	n=1	n=1	
	Stress - Elongation	n=1	n=1		
	Temperature - Elongation	n=1	n=1		
ACFR	Appearance and structure	n=3	n=1	n=1	n=1
	Cross-section	n=6	n=2	n=2	n=2
	Tensile load, electrical resistance	n=1	n=1		
	Stress - Elongation	n=1	n=1		
	Temperature - Elongation	n=1	n=1		

* The test items are appearance, structure, tensile load, elongation, and electrical conductivity.

Table IV Test items and quantities for compression clamps

Sample	Test Items	Test quantity
Compression clamp	Appearance	n=3
	Cross-section	n=1
	Tensile load	n=2
	Electrical resistance	n=3

3.2 Results of performance verification tests of conductor

3.2.1 Appearance, structure, and cross-sectional testing

Fig. 3 shows the CFCC at the lowest part of the sag. No abnormality such as damage or corrosion was observed at the lowest part of the sag and the gripping area of the suspension clamp and the damper. Fig. 4 shows the ACFR cross section at the lowest part of the sag. No accumulation of corrosion products or decrease in cross-sectional area was observed in the conductor.



Fig. 3 CFCC at the lowest part of the sag

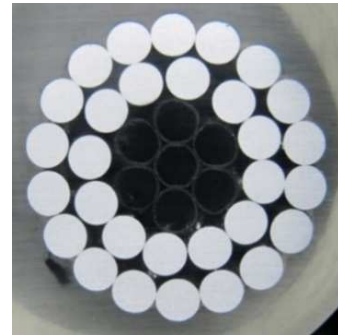


Fig. 4 ACFR cross section at the lowest part of the sag

3.2.2 Tensile load test

The results of tensile load test of CFCC are shown in Table V. Both the breaking load and the load at 1% elongation satisfied the standard values and were almost the same as the initial values. The tensile load test results of ACFR are shown in Fig. 5. The measured value of 79.0 kN satisfied the standard value of 68.9 kN. Compared with the initial value of 79.3 kN, the difference was less than 1%, and there was almost no performance degradation. The tensile load was almost the same as the initial value, and from the tendency of a slight decrease in tensile load, it is concluded that the ACFR can be used without any problem during the service life of the transmission facility.

Table V Tensile load test results for CFCC

Item	Standard value	Test results	Initial value (2002)
Breaking load	57.0 kN or more	71.8 kN	74.9 kN
Load at 1% elongation	38.9 kN or more	42.2 kN	41.8 kN

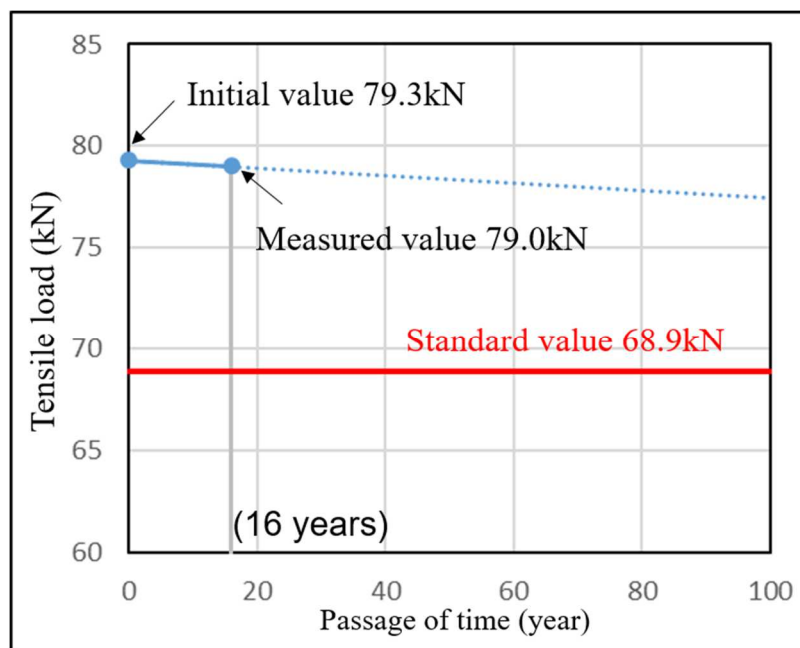


Fig. 5 Results of ACFR tensile load test

3.2.3 Electrical resistance test

Table VI shows the results of the electrical resistance test of ACFR. The electrical resistance of 0.183-0.184 Ω/km is almost equal to the calculated value of 0.182 Ω/km or less. As shown in Table VII, the electrical conductivity test results of the hard aluminum strands were between 61.6% and 62.4%, which is well within the standard value of 61% or higher, and therefore, no deterioration in electrical performance was observed.

Table VI Electrical resistance test results for ACFR

Item	Electrical resistance (Ω/km at 20 °C)
Calculated value	0.182 or less
First time	0.184
Second time	0.184
Third time	0.183

Table VII Conductivity test results of hard aluminum strands

Item	Conductivity (%)
Standard value	61 or more
Maximum value	62.4
Minimum value	61.6
Average value*	62.1

*Average value of n=30 aluminum strands

3.2.4 Stress- elongation test

The stress-elongation test results of ACFR are shown in Fig. 6. In this figure, no significant inflection point was observed. The measured results of modulus of elasticity for CFCC and ACFR are shown in Table VIII. The modulus of elasticity of CFCC was almost the same as the calculated value and initial value. Meanwhile, the modulus of elasticity of ACFR was almost the same as that of the initial value, although it was lower than the calculated value.

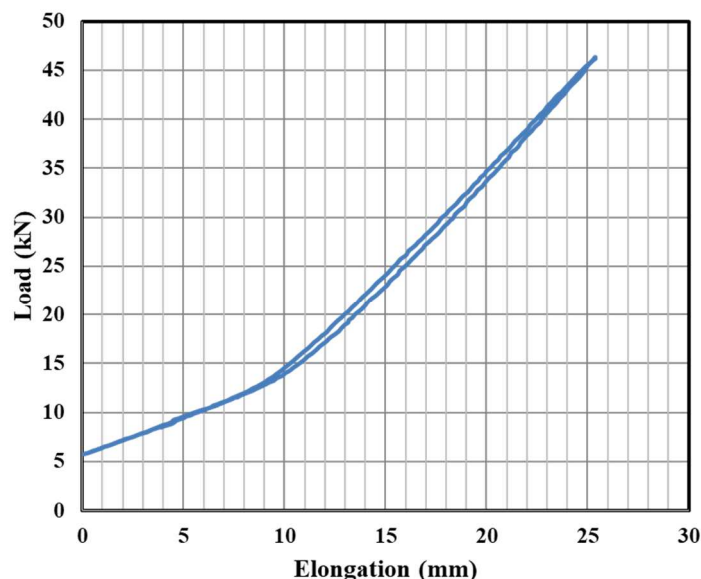


Fig. 6 Stress-elongation test results for ACFR

Table VIII Modulus of elasticity for CFCC and ACFR

Sample	Calculated value	Measured value	Initial value (2002)
CFCC	137 GPa	139 GPa	142 GPa
ACFR	76.0 GPa	63.0 GPa	60.2 GPa

3.2.5 Temperature-elongation test

The temperature-elongation relationship of ACFR is shown in Fig. 7. In this figure, it can be seen that up to 90°, the thermal expansion coefficient is the sum of CFCC and aluminum conductor, and above that temperature, the aluminum conductor elongates more. Consequently, the shared stress becomes zero, and the thermal expansion coefficient depends on CFCC alone. The thermal expansion coefficient of CFCC and ACFR are shown in Table IX. The thermal expansion coefficients of CFCC and ACFR are negative above the transition point temperature, but this is not abnormal because it is widely known that the thermal expansion coefficient of polyacrylonitrile (PAN)-based carbon fiber, which is the material of CFCC, is negative.

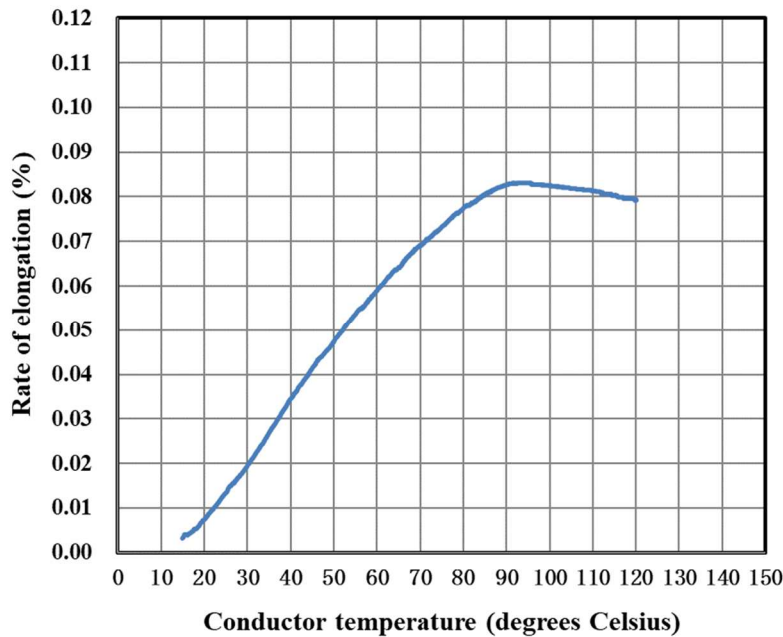


Fig. 7 Temperature-elongation characteristics of ACFR

Table IX Thermal expansion coefficient of CFCC and ACFR

Sample	Calculated value	Measured value	Initial value (2002)
CFCC	$1.0 \times 10^{-6}/^{\circ}\text{C}$	$-1.6 \times 10^{-6}/^{\circ}\text{C}$	$0.7 \times 10^{-6}/^{\circ}\text{C}$
ACFR	$15.5 \times 10^{-6}/^{\circ}\text{C}$	$12.4 \times 10^{-6}/^{\circ}\text{C}$ (Above transition point : $-1.6 \times 10^{-6}/^{\circ}\text{C}$)	$20.5 \times 10^{-6}/^{\circ}\text{C}$

3.3 Performance evaluation test results of the compression-type dead-end clamp

Performance evaluation tests were conducted on the compression clamps that had been used with ACFR for 16 years [3].

3.3.1 Appearance and cross-sectional test

In the appearance test, there were no harmful rust, cracks, or other defects. In the cross-sectional survey, no abnormalities such as broken conductors or corrosion were observed for the aluminum conductor and CFCC inside the clamp. Fig. 8 shows ACFR inside the aluminum clamp, and Fig. 9 shows CFCC inside the aluminum clamp.



Fig. 8 ACFR inside the aluminum clamp



Fig. 9 CFCC inside the aluminum clamp

3.3.2 Tensile load test

The results of the tensile load test are shown in Fig. 10. Both samples satisfied the standard values, and no degradation over time was observed. In the case of sample No. 1, the load got lowered once during the test, which is presumed to be due to the slippage of the conductor inside the test fixture.

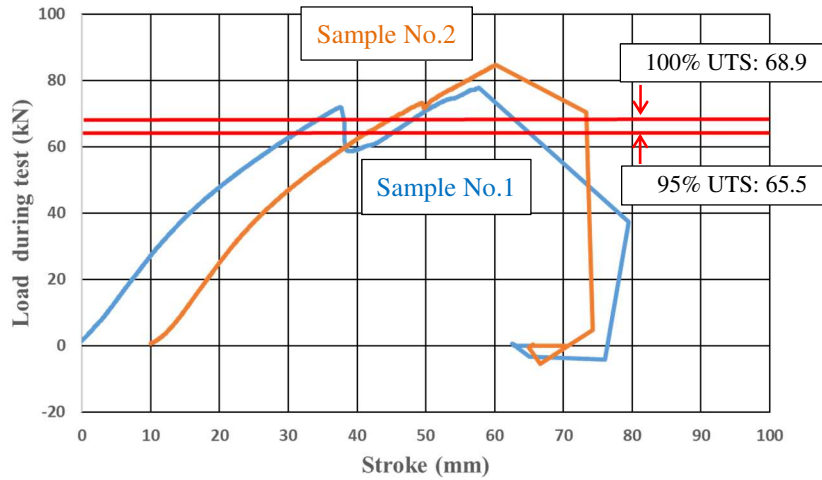


Fig. 10 Results of tensile load test

3.3.3 Electrical resistance test

The results of the electrical resistance test for sample No. 1 are shown in Table X and the measurement locations are shown in Fig. 11. The electrical resistance at each measurement point was less than 100% of the elect the applicable conductor, confirming that there was no problem. The tendency of Load during test (kN) samples No. 2 and No. 3 were almost the same as for sample No. 1.

Table X Electrical resistance test results

Sample	Measured point	Measured distance L (mm)	Conductor standard value (Ω/km at 20°C)	Measured value (Ω/km at 20°C)	Conductor to conductor Resistance ratio (%)
No.1	A	650	0.182	0.044	24.2
	B	215		0.085	46.7
	C	150		0.082	45.1
	Overall	1015		0.060	33.0

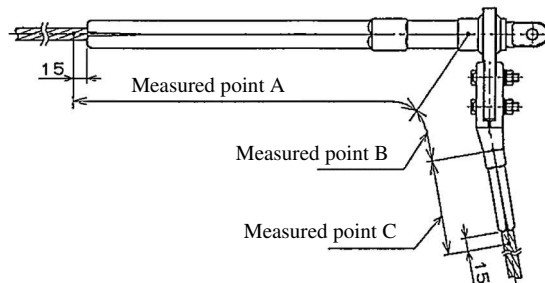


Fig. 11 Measurement locations

4. TECHNOLOGICAL DEVELOPMENT TO EXPAND THE APPLICATION OF ACFR

In order to expand the application of ACFR, an SBTACFR and a compression-type dead-end clamp that passes through a sheave were developed, and counterweights and Christmas tree-shaped dampers were verified for application.

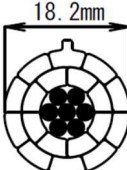
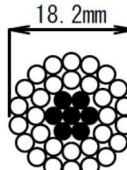
4.1 SBTACFR

In order to expand the application of ACFR to actual lines, the authors have developed SBTACFR (SB: Smooth Body), in which the aluminum strand is formed into a trapezoidal shape to enlarge the cross-sectional area of the aluminum portion, thus reducing power losses and increasing the transmission capacity. Table XI shows the conductor specifications of SBTACFR 190 mm², and Table XII compares SBTACFR with TACSR and ACSR. Comparing the continuous allowable currents of ACSR 160 mm² and SBTACFR 190 mm², which have the same wire outer diameter, the allowable current for TACSR can be increased by about 76%.

Table XI Conductor specifications of SBTACFR 190 mm²

Item		Unit	SBTACFR 190 mm ²
Strand configuration	Aluminum strand	Number/mm	1/4.14+9/3.82+8/3.52
	Core strand		7/2.6 CFCC
Tensile load (UTS)		kN	79.5
Outer diameter	Conductor	mm	18.2
	Core	mm	7.8

Table XII Comparison of SBTACFR with TACSR and ACSR

	SBTACFR 190 mm ²	TACSR 160 mm ²	ACSR 160 mm ²
Allowable continuous current	800 A	705 A	454 A
Conductor cross section			

4.2 Sheave passing compression-type dead-end clamp

The compression-type dead-end clamp for ACFR developed so far was a one-piece type that grips the outer layer of the conductor only with an aluminum clamp to prevent the CFCC from being crushed by the steel compression clamp. However, securing the force to grip the conductor requires the aluminum clamp to be long, which, in turn, requires a long time for installation. To solve this, an aluminum tube was inserted between the outer layer of the conductor and the steel clamp as a cushioning material to reduce the compression force against the CFCC; this has enabled the steel clamp to grip the conductor without the risk of crushing, and consequently, the shortened clamp with the reduced gripping area improves work performance. The structure of a newly developed sheave passing compression-type dead-end clamp is shown in Fig. 12. This clamp can pass through the sheave after being installed on the conductor by compression. It can be applied for the prefabricated stringing method. This method measures the length of a conductor and installs the dead-end clamp on it by compression on the ground in advance then does aerial work for stringing the conductor, thus reducing the work time required for compression on the tower.

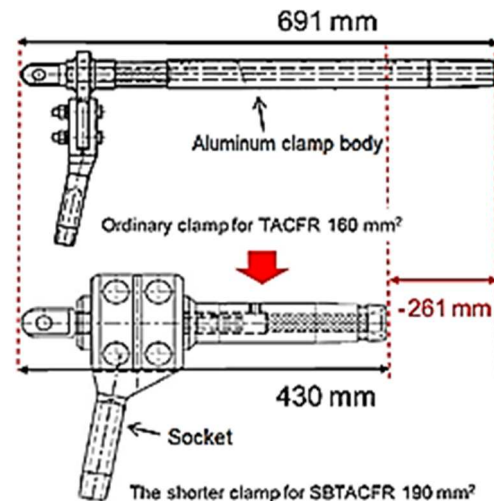


Fig. 12 Structure of the sheave passing compression-type dead-end clamp

4.3 Counterweight

The structure of a counterweight is shown in Fig. 13. This counterweight was designed to suppress heavy snow accumulation on overhead lines. One of the factors that cause heavy snow accumulation is considered to be "rotation of the transmission line due to the twisting moment generated by the snow on the transmission line. This counterweight reinforces the torsional rigidity of the conductor and suppresses the rotation of the conductor. We conducted a torsional stiffness test to see if it was possible to use the same counterweight for existing conductors that have the same shape as the ACFR, and confirmed that the counterweight was effective for ACFR in preventing torsion. In addition, various performance verification tests, such as conductor swaying tests, were conducted, and it was confirmed that there was no problem.

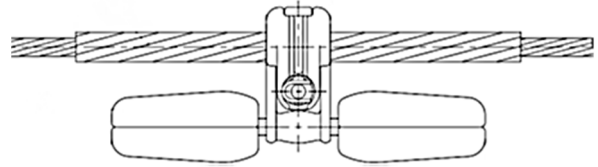


Fig. 13 Structure of counterweight

4.4 Anti-vibration damper

The structure of a Christmas tree-shaped damper is shown in Fig. 14. This damper is a type of anti-vibration damper and is designed to suppress the wind vibration of transmission lines. From the tests conducted previously by the authors, the ACFR was known to have low vibration absorption energy; thus, because of its high vibration isolation characteristics, the Christmas tree-shaped damper was chosen.

Since there had been no damper for existing conductors with the same shape as ACFR, we designed a new damper and conducted vibration isolation characteristic tests, and confirmed that the new damper was effective in suppressing wind vibration. In addition, various performance verification tests, such as vibration fatigue tests, were conducted and confirmed that there was no problem.

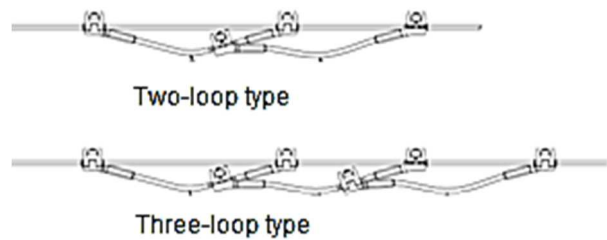


Fig. 14 Structure of Christmas tree-shaped damper

5. CONCLUSION

The authors collected samples from ACFR and compression-type dead-end clamps, which had been in-service near the coastline for 16 years, and carried out various performance evaluation tests. The test results show that no significant degradation was observed, and since there was only a slight decrease in tensile load, it indicates that ACFR could be used without any problem during the service life of transmission facilities. Consequently, this demonstrates the reliability of ACFR during the long-term service of overhead transmission lines. Furthermore, to expand the application of ACFR, the authors developed an SBTACFR which is capable of reducing power losses and increasing the transmission capacity, and verified the sheave passing compression-type dead-end clamp, counterweights, and the anti-vibration damper for application. As a result, the expansion of the application of ACFR has been foreseen.

BIBLIOGRAPHY

- [1] S. Ueda, C. Nascimento, M. Takayama, "Flexible HTLS – High Temperature Low Sag Conductor", (CIGRE SESSION PARIS 2020 B2-201, page 4)
- [2] F. Sato, H. Ebiko, "DEVELOPMENT OF A LOW SAG ALUMINUM CONDUCTOR CARBON FIBER REINFORCED FOR TRANSMISSION LINES", (CIGRE SESSION PARIS 2002 22-203, pages 2-3)
- [3] Working Group B2.32 CIGRE, "Technical Brochure on Evaluation of Aged Fittings" (CIGRE Technical Brochure 477, October 2011, pages 11-20).